

A FLEXIBLE GEOMETRIC WIDE-BAND TIME-VARYING CHANNEL MODEL FOR V-BLAST MIMO SIMULATIONS

Steve Gifford, John E. Kleider and Scott Chuprun
General Dynamics, Decision Systems, Scottsdale, AZ
Steve.Gifford@gd-decisionssystem.com

ABSTRACT*

This paper presents a geometrically based channel model that provides robust channel simulations for wide-band waveforms such as multiple-input multiple-output (MIMO), multi-user detection (MUD) and orthogonal frequency division multiplexing (OFDM) communication waveforms. The model supports multiple transmit and receive antennas, multiple multipath reflectors, and mobility for Rayleigh fading environments with frequency-selective fading as well as time-selective fading. For static testing, the model supports the pseudo-stationary channel, which is helpful for initial testing of communication waveforms. This channel model is ideal for testing of MIMO communications systems, which require a rich scattering environment. This paper presents results of V-BLAST (Vertical Bell Laboratories Layered Space-Time) MIMO simulations using the geometric channel model with pseudo-stationary and Rayleigh fading environments. MIMO architectures such as V-BLAST can be easily implemented by exploiting the built-in and flexible multi-channel architectures of advanced Software Defined Radios (SDR).

1. INTRODUCTION

Recent research has shown that a rich scattering environment is capable of significant communication capacity due to the multipath diversity inherent in the rich scattering environment. MIMO techniques, such as V-BLAST, have demonstrated spectral efficiencies of 20-40 bps/Hz in an indoor environment [1]. Consequently, a lot of interest has developed in MIMO systems. Simulation testing for MIMO or other smart antenna applications requires a chan-

nel model that is extensively more complicated than those used for single-input single-output (SISO) systems. Early channel models were narrow-band and provided only information about the statistics of the received signal amplitude and Doppler shifts of the spectrum [2]. Modern communication techniques such as MIMO, MUD, smart antennas and others require wideband models of the channels with multiple transmit and receiving antennas and many multipath reflectors to adequately model the effects of the actual communication channel. Several improved channel models have been devised. These include the Geometrically Based Single Bounce Elliptical Model (GBSBEM) [3] and the Geometrically Based Single Bounce Macrocell (GBSBM) model [4] that provides statistical estimates of the angle of arrival (AOA), Doppler spectrum and fading envelopes. The model that we choose to implement most closely follows that of Liberti's GBSBEM [3]. The model also is similar to ray tracing models developed by Fette [5] and Valenzuela [6]. Our model is referred to as the Geometric Wide-band Time-varying Channel Model (GWTCM). The GWTCM uses an elliptical boundary to limit multipath spread, implements wideband channel modeling by partitioning the spectrum into multiple flat channels, provides for mobility of objects and can calculate the AOA and fading envelopes from the received signal. The GWTCM uses a single bounce model for the multipath components but can be extended to more reflections to reduce the standard deviation of the prediction error [7]. The geometrical nature of the GWTCM model also allows experimentation with MIMO phenomena such as keyholes and correlated multipath [8].

This paper is organized as follows. Section 2 provides a description of the GWTCM channel model with examples of the rich channel environment that can be modeled. Section 3 provides a discussion of the theory of MIMO-OFDM using V-BLAST. Section 4 provides simulation results for V-BLAST-OFDM when using a Rayleigh fading environment. Conclusions are provided in section 5.

Prepared through collaborative participation in the Communications and Networks Consortium sponsored by the U.S. Army Research Laboratory under the Collaborative Technology Alliance Program, Cooperative Agreement DAAD19-01-2-0011. The U.S. Government is authorized to reproduce and distribute reprints for Government purposes notwithstanding any copyright notation thereon. The views and conclusions contained in this document are those of the authors and should not be interpreted as representing the official policies, either expressed or implied, of the Army Research Laboratory or the U.S. Government.

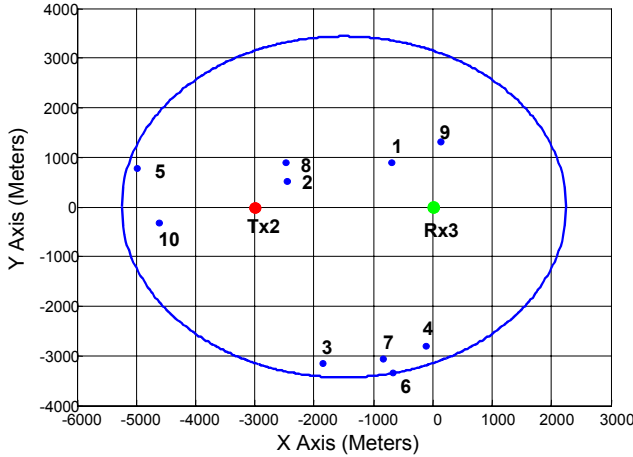


Figure 1. 3x2 MIMO Geometry

2. THE GWTCM CHANNEL MODEL

Figure 1 shows an example of the GWTCM geometry that we used for a 3x2 MIMO communications system consisting of $M=3$ isotropic receive antennas and $N=2$ isotropic transmit antennas. $K=10$ multipath reflectors are placed inside of an ellipse that represents the loci of multipath reflectors with a multipath delay of $\tau_m = 25 \mu\text{sec}$. The elliptical channel model ignores multipath delays larger than τ_m since very long delays have higher path loss and thus do not contribute substantially to the received power [2]. Given a specific time varying geometry, our goal is to calculate the wideband frequency-domain transfer function, H , between the M receive antennas and the N transmit antennas as a function of time and frequency. The following assumptions are made:

1. OFDM divides the bandwidth, W , into flat narrowband subcarriers, with subcarrier bandwidth, f_s .
2. The OFDM waveform uses a cyclic or null extension that equals or exceeds the multipath delay spread, τ_s , so that intersymbol interference (ISI) does not occur.
3. The sampling period, T_s , is the OFDM symbol time.
4. The velocities of components are constant over T_s .
5. The Doppler components, due to velocity, are sufficiently small, such that they do not destroy the orthogonality of the OFDM subcarriers.
6. All antennas and multipath reflectors have an isotropic radiation pattern.
7. All antennas have an identical polarization.

The task of calculating H is simplified by breaking down the MIMO model into multiple simplified SISO models as depicted in Figure 2. $M \times N$ line of sight (LOS) and $M \times N \times K$ multipath components exist.

The LOS power received at antenna m from transmit antenna n is [2]:

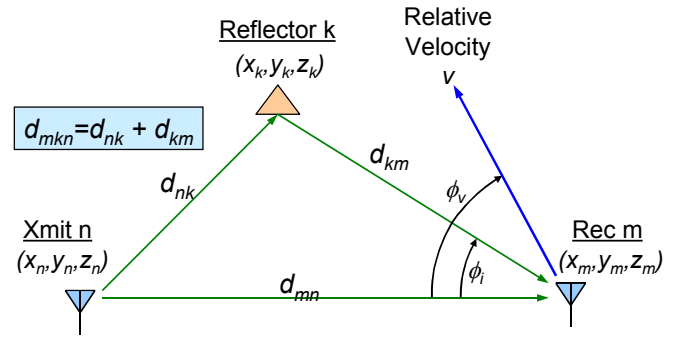


Figure 2. SISO Geometry

$$P_{mn} = P_{ref} - 10p \log\left(\frac{d_{mn}}{d_{ref}}\right) + G_r(0) + G_t(0) - L_d \quad (1)$$

where P_{mn} and P_{ref} are in dBm, p is the exponential path loss factor, d_{mn} is the geometric distance in meters from transmitter n to receiver m , d_{ref} is the reference distance at which P_{ref} is measured, $G_r(0)$ is the gain of the receive antenna in the direction of the transmitter and $G_t(0)$ is the gain of the transmit antenna in the direction of the receiver. The gains, $G_r(0)$ and $G_t(0)$, are 0 dB since we are using isotropic antennas. L_d is a parameter that has been added to provide indirect control of the direct path losses for flexible MIMO testing. P_{ref} is the reference power that is measured at a distance $d_{ref} = 1$ meter where P_{ref} for an isotropic antenna is

$$P_{ref} = P_T - 20 \log\left(\frac{4\pi d_{ref}}{C}\right) \quad (2)$$

where P_T is the transmitted power in dBm and C is the speed of light. The receive signal due to the direct path is

$$r_{mn} = A_{mn} e^{\frac{-j2\pi d_{mn}}{\lambda_{mn}}} \quad (3)$$

where A_{mn} represents the linear magnitude of a signal with power P_{mn} , and λ_{mn} is the direct path wavelength observed at receive antenna m for the signal transmitted on antenna n .

The received power for the k^{th} multipath component on receive antenna m from transmit antenna n is

$$P_{mkn} = P_{ref} - 10p \log\left(\frac{d_{mkn}}{d_{ref}}\right) - L_r + G_r(\theta_k) + G_t(\phi_k) \quad (4)$$

where P_{mkn} is in dBm, d_{mkn} is the geometric distance from m to k to n . L_r represent the loss in dB due to reflection from the multipath reflector k , $G_r(\theta_k)$ is the receiver antenna gain as a function of the direction of arrival, and $G_t(\phi_k)$ is the

gain of the transmitting antenna in the direction of depar-

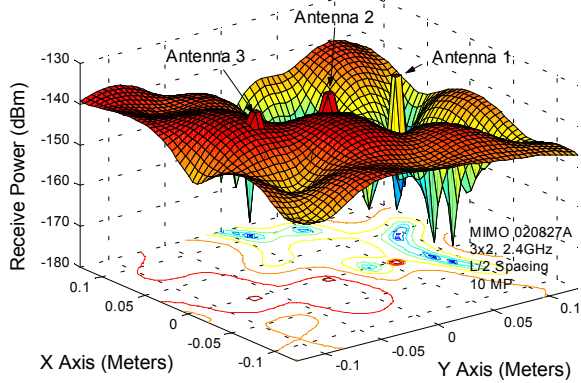


Figure 3. 3x2 MIMO Receive Power for $P_T=0$ dBm

ture. The gain factors, $G_r(\theta_k)$ and $G_r(\phi_k)$, are 0 dB since we are dealing with isotropic antennas.

The received signal from multipath component k is

$$r_{mkn} = B_{mkn} e^{\frac{-j2\pi d_{mkn}}{\lambda_{mkn}}} \quad (5)$$

where B_{mkn} represents the linear magnitude of a signal with power P_{mkn} and where λ_{mkn} is the wavelength at receive antenna m due the multipath signal, k , from transmit antenna, n .

The transfer function, $H(m, n, t, f_s)$, where t is the OFDM frame number and f_s is the subcarrier frequency, is thus the component due to the direct path as shown in (3) and the summation of K multipath components as shown in (5)

$$H(m, n, t, f_s) = A_{mn} e^{\frac{-j2\pi d_{mn}}{\lambda_{mn}}} + \sum_{k=1}^K B_{mkn} e^{\frac{-j2\pi d_{mkn}}{\lambda_{mkn}}} \quad (6)$$

For the case of mobile receive antenna m and static transmit antenna n and multipath reflector k , as shown in Figure 2, the doppler shift, v_{mkn} , can be found by [2]

$$v_{mkn} = \frac{v}{\lambda_s} \cos(\phi_i - \phi_v) \quad (7)$$

where v is the velocity of receive antenna m , λ_s is the wavelength of subcarrier frequency, f_s , ϕ_i is the AOA at receive antenna n , and ϕ_v is the relative angle of travel for receive antenna n . The receive frequency, f_m , at antenna m , is thus

$$f_m = f_s + v_{mkn} \quad (8)$$

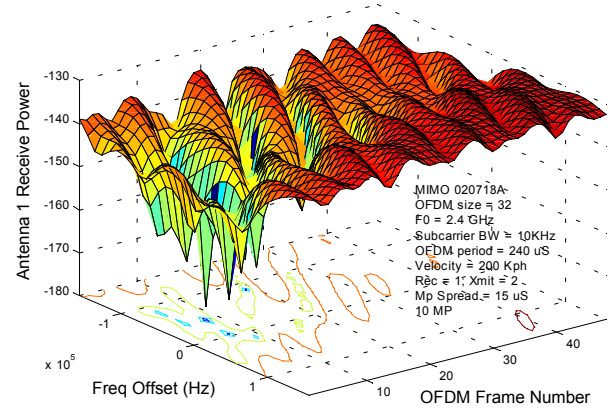


Figure 4. MIMO-OFDM Time-Frequency Plane

then the received wavelength, λ_{mkn} is

$$\lambda_{mkn} = \frac{c}{f_m} \quad (9)$$

The wavelength of the direct path, λ_{mn} , is found in a similar manner.

Figure 3 shows the receive power surface for the area near the three isotropic receive antennas for the case where the transmit power, P_T , is 0 dBm. The receive antenna array used a spacing of $\lambda/2$ at an operating frequency of 2.4 GHz and the transmit array used a spacing of 10 meters. Reference locations for the three receive antennas are shown by the large peaks. The power received at each antenna is determined by where the antenna pokes through the undulating surface. Note that very small displacements of the antennas may place them in deep nulls.

The plot in Figure 4 shows the antenna 1 receive power as a function of frequency and OFDM frame number for the case where the transmit power, P_T , for transmit antenna, $n = 2$, is 0 dBm, and the transmit array moved in the NE direction with a velocity, $v = 200$ Kph. The geometry of the experiment is shown in Figure 1. An OFDM size of 32 with a center frequency of 2.4 GHz was used. The OFDM subcarrier bandwidth was 10 KHz and the OFDM symbol time was 240 usec. Note the deep time and frequency selective fades at OFDM frame number 8 in Figure 4.

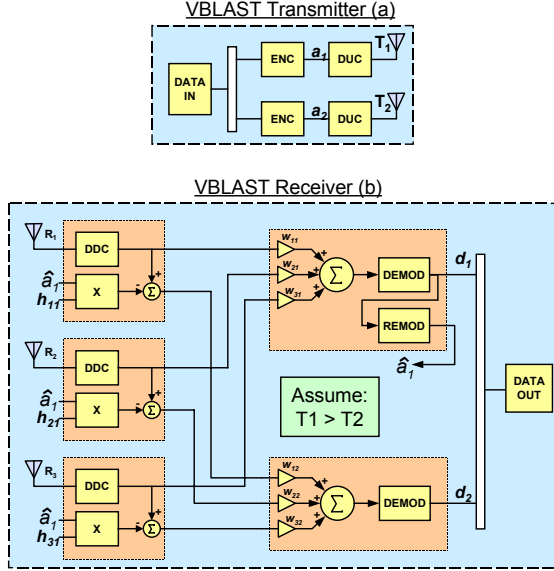


Figure 5. 3x2 V-BLAST Architecture

3. MIMO-OFDM V-BLAST

The GWTCM channel model was created to help test and evaluate MIMO communication systems. The MIMO technique that we have concentrated on is the V-BLAST algorithm [1]. V-BLAST was developed a few years ago and demonstrated previously unachieved spectral efficiencies of 20-40 bps/Hz in a lab environment. MIMO techniques rely on a rich scattering environment to provide multipath diversity such as that found in many wireless environments. The phenomenal channel capacities of MIMO grow linearly with the number of antenna and nearly approach the theoretical Shannon capacity limit. We implemented an OFDM version of V-BLAST by independently processing each OFDM subcarrier using a conventional V-BLAST architecture. A block diagram of a conventional 3x2 V-BLAST system is shown in Figure 5. Given a specific OFDM frame number, t , and a specific OFDM subcarrier frequency, f_s , the V-BLAST process is defined as follows: The input data is separated into two data streams and independently encoded to form symbols a_1 and a_2 . Let the baseband transmitted symbols be represented by $\mathbf{a} = [a_1, a_2]^T$. The encoding may consist, for example, of gray coded QPSK. The symbol set \mathbf{a} is then upconverted and transmitted using transmit antennas T_1 and T_2 . The baseband receive signal assuming zero frequency offset is

$$\mathbf{r}_1 = H_{sub} \mathbf{a} + \mathbf{v} \quad (10)$$

where \mathbf{r}_1 represents the $M \times 1$ receive vector for the receive antenna array, H_{sub} is the $M \times N$ channel matrix consisting of complex scalars, and \mathbf{v} is a complex additive white Gaussian noise (AWGN) vector. Recall that the wideband time

varying model developed in Section 2 is a function of the m^{th} receive antenna, the n^{th} transmit antenna, the t^{th} OFDM frame number and subcarrier frequency f_s . H_{sub} represents the flat fading channel coefficients for the given OFDM frame number, t , and OFDM subcarrier frequency, f_s as

$$H_{sub}(m, n) = H(m, n, t, f_s) \quad (11)$$

Assume that the noise, \mathbf{v} , is zero, for the purposes of understanding the receive process. For our 3x2 V-BLAST example in Figure 5, the goal of the receiver is to accurately estimate the transmitted symbols a_1 and a_2 . This may seem difficult since the energy in a_1 and a_2 are the same for QPSK modulation. The V-BLAST receiver uses two powerful signal processing algorithms. The first, is called zero-forcing nulling and is used by the receive array to *reject* the signal *not* of interest. The second algorithm, is successive interference cancellation (SIC), that is used to separate the signals a_1 and a_2 once either a_1 or a_2 is estimated. The V-BLAST receive algorithm for the 3x2 MIMO system shown in Figure 1 is summarized below:

1. Find the strongest transmitted signal, either the signal transmitted from T_1 or T_2 . Assume for the purposes of this discussion that T_1 has the dominant signal strength. Also assume that we have perfect knowledge of H .
2. Apply an antenna array nulling signal, w_1 , to null out the T_2 signal.
3. Demodulate the received energy and output data estimate, d_1 .
4. Re-modulate the data estimate, d_1 , and obtain transmitter T_1 symbol estimate \hat{a}_1 .
5. Now that we have an estimate of a_1 and knowledge of the channel, H , we can use SIC to subtract out the signal T_1 from each of the receive antennas. Compute the receive vector for the signal transmitted on T_2 :

$$\mathbf{r}_2 = \mathbf{r}_1 - \hat{a}_1 H_1 \quad (12)$$

where $H_1 = [h_{11} \ h_{21} \ h_{31}]^T$.

6. Apply spatial receive filter, w_2 , to signal \mathbf{r}_2 .
7. Demodulate the signal and output data estimate, d_2 .

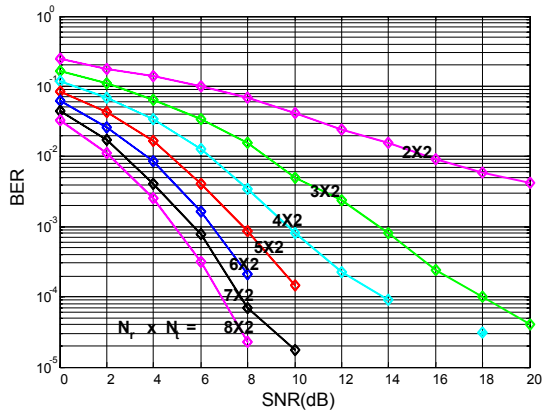


Figure 6. Mx2 V-BLAST Performance

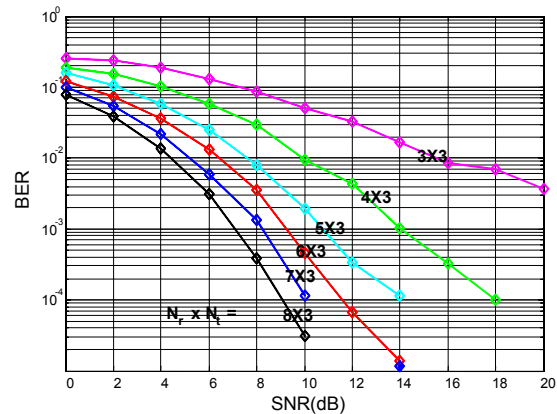


Figure 7. Mx3 V-BLAST Performance

4. SIMULATION RESULTS

An experiment was performed to verify the performance of the V-BLAST algorithm. The experiment consisted of a single carrier at 2.4 GHz modulated with gray coded QPSK and the channel model was configured to implement Rayleigh fading. We choose to use a traditional stochastic Rayleigh channel model to test the V-BLAST algorithm so that the results could be compared with published curves. Results for the GWTCM model are highly dependent on the geometry and other model parameters. Future research paper will present results from the GWTCM model. For these experiments, the Rayleigh channel matrix, H , is of the form (for 3x2):

$$H = \begin{bmatrix} h_{11} & h_{12} \\ h_{21} & h_{22} \\ h_{31} & h_{32} \end{bmatrix} \quad (13)$$

where each flat Rayleigh fading coefficient is formed by summing a real and an imaginary Gaussian random variable that have independent and identically distributed (i.i.d.) statistics. Results for the Mx2 case are shown in Figure 6.

The next experiment consisted of measuring the performance of Mx3 V-BLAST systems. Figure 7 shows the results of this test. Note that when comparing the Mx2 results in Figure 6 and the Mx3 results in Figure 7, that the Mx3 systems have degraded performance. This is due to the ability of the receiver to provide improved nulling and canceling for the Mx2 case compared to the Mx3 case. The Mx3 case is similar to having two undesired users occupying the same signal bandwidth as the desired signal. For the Mx2 case, there is only one interfering signal as opposed to two in the Mx3 case.

The next experiment shows the MxM performance of V-BLAST systems. Figure 8 shows the results of this experiment. Note that the performance of the MxM system improves as M gets smaller. Also note that the BER performance for large values of M seems to asymptotically approach a boundary.

5. CONCLUSION[#]

This paper has presented the design of a geometrically based time-varying channel model that provides robust channel simulations for wideband waveforms such as MIMO and MUD. The channel model supports multiple transmit and receive antenna and multiple multipath reflectors. The model supports mobility for Rayleigh fading environments as well as time and frequency selective fading. MIMO architectures such as V-BLAST can be easily implemented by exploiting the built-in and flexible multi-channel architectures of advanced SDR's.

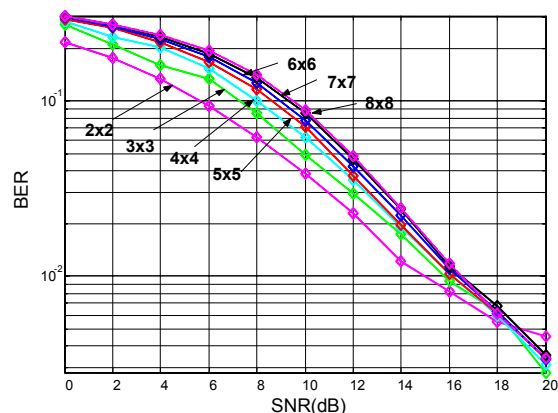


Figure 8. MxM V-BLAST Performance

[#] The views and conclusions contained in this document are those of the authors and should not be interpreted as representing the official policies, either expressed or implied, of the Army Research Laboratory or the U.S. Government.

6. REFERENCES

- [1] P.W. Wolniansky, G.J. Foschini, G.D. Golden, and R.A. Valenzuela, "V-BLAST: An Architecture for Realizing Very High Data Rates Over the Rich-Scattering Wireless Channel," *Proc. Int. Symposium on Advanced Radio Technologies*, Boulder, CO, Sept. 10, 1998.
- [2] J.C. Liberti and T.S. Rappaport, *Smart Antennas for Wireless Communications*, Prentice Hall, Upper Saddle River, NJ, 1999.
- [3] J.C. Liberti and T.S. Rappaport, "A Geometrically Based Model for Line-of-Sight Multipath Radio Channels", *IEEE Vehicular Technology Conf.*, pp. 844-848, Apr. 1996.
- [4] P. Petrus, J.H. Reed, and T.S. Rappaport, "Geometrically based statistical channel model for macrocellular mobile environments," *Global Telecommunications Conference*, Vol. 2, pp. 1197-1201, 1996.
- [5] B. Fette, "A Ray Tracing Model of Radio Frequency Propagation," *Internal Technical Paper, General Dynamics-Decision Systems*, 1991.
- [6] R.A. Valenzuela, "Ray tracing prediction of indoor radio propagation," *Personal, Indoor and Mobile Radio Communications*, pp. 140-144, Vol. 1, 1994.
- [7] R.A. Valenzuela, S. Fortune, and J. Ling, "Indoor propagation prediction accuracy and speed versus number of reflections in image-based 3-D ray-tracing," *Vehicular Technology Conference*, Vol. 1, 1998.
- [8] D. Chizhik, G.J. Foschini, M.J. Gans, and R.A. Valenzuela, "Keyholes, Correlations, and Capacities of Multielement Transmit and Receive Antennas," *IEEE Trans. on Wireless Communications*, Vol. 1, pp. 361-368, April 2002.